Evaluation of an Anatomical Based MAP Reconstruction Algorithm for PET in Epilepsy

Kristof Baete, *Student Member, IEEE,* Johan Nuyts, *Member, IEEE,* Wim Van Paesschen, Paul Suetens, *Member, IEEE,* and Patrick Dupont

***Abstract*— We studied the performance of our anatomical based maximum-a-posteriori reconstruction algorithm (A-MAP) for the detection of hypo-metabolic regions in positron emission tomography (PET) of the brain of epilepsy patients [1]. Between seizures, 2-[^{18}F]fluoro-2-deoxy-D-glucose PET shows a decreased glucose metabolism in gray matter (GM) associated with the epileptogenic region. However, detection of these regions is limited by noise in the measurement and the relatively small thickness of GM compared to the spatial resolution of PET. We hypothesize that incorporating anatomical information, derived from magnetic resonance imaging data, and pathophysiological knowledge in the reconstruction process improves the detection of hypo-metabolic regions. Monte-Carlo based brain software phantom experiments were used to examine the performance of A-MAP. The influence of small mis-registration errors of the anatomical information and weight of the a priori information in GM were studied. A-MAP showed improved results for signal-to-noise ratio, bias and variance. As an illustration, clinical PET data of an epilepsy patient was reconstructed using A-MAP and post-smoothed maximum-likelihood. We can conclude that the use of anatomical and pathophysiological information during the reconstruction process is promising for the detection of subtle hypo-metabolic regions in the brain of patients with epilepsy.**

I. Introduction

POSITRON emission tomography (PET), with the use of 2-[^{18}F]fluoro-2-deoxy-D-glucose (FDG), often shows a decreased cerebral glucose metabolism between seizures in gray matter (GM) areas associated with the epileptogenic region. These hypo-metabolic regions can be difficult to detect. Part of the detection problem is due to the partial volume effect (PVE) caused by the limited spatial resolution of PET. Unfortunately, PVE can lead to spurious hypo-metabolic regions.

We hypothesized that anatomical information, derived from magnetic resonance imaging data, and patho-physiological knowledge in the reconstruction process improves the detection of hypo-metabolic regions. For that purpose, an anatomical based maximum-a-posteriori reconstruction algorithm (A-MAP) has been developed [1]. In this study, we make an evaluation of this iterative reconstruction algorithm.

II. Methods

If no lesions or tumors are present, one can reasonably assume that for FDG-PET white matter (WM) activity is approximately uniform and cerebrospinal fluid (CSF) activity is approximately zero. GM, WM and CSF can be identified using high-resolution magnetic resonance (MR) imaging data. Segmentation algorithms can accurately determine the probability that a voxel belongs to a certain tissue class. We assume that this probability approximates tissue composition and use it as a tissue fraction. The set of segmentation images are $\{f^G, f^W, f^C, f^O\}$, with O the class "other".

For an activity distribution $\Lambda = \{\lambda_j\}$ in a PET scanner, y_i photon pairs are measured at line of response i. If λ_j is the activity at voxel j and c_{ij} the probability that photons emitted in j were detected in i, then the expected amount of photon pairs is $E(y_i) = \sum_j c_{ij}\lambda_j$. System matrix $\{c_{ij}\}$ describes the projection process with associated physical effects that take place between emission and detection. We include photon attenuation and the finite detector resolution effect. Scatter and randoms are ignored in the theoretical framework.

We define subsets of $\mathbb{J} = \{j\}$ based on the segmentations:

$$\mathbb{B} = \{j \in \mathbb{J} \,|\, f_j^G + f_j^W + f_j^C > 0.01\} \quad (1)$$

$$\mathbb{G} = \{j \in \mathbb{B} \,|\, f_j^G > 0.01\} \quad (2)$$

$$\mathbb{W} = \{j \in \mathbb{B} \setminus \mathbb{G} \,|\, f_j^W > 0.99\} \quad (3)$$

$$\mathbb{C} = \{j \in \mathbb{B} \setminus \mathbb{G} \,|\, f_j^C > 0.99\} \quad (4)$$

Every voxel can be thought of as the total amount of fractional activities of the contributing tissues, or

$$\lambda_j = f_j^G\lambda_j^G + f_j^W\lambda_j^W + f_j^C\lambda_j^C + f_j^O\lambda_j^O \quad (5)$$

We can approximate this equation with

$$\lambda_j \approx f_j^G\lambda_j^G + f_j^W\bar{\lambda}^W + f_j^C\bar{\lambda}^C \quad (6)$$

for all $j \in \mathbb{G}$, with $\bar{\lambda}^W$ the mean activity in $\mathbb{W}$ and $\bar{\lambda}^C$ the mean activity in $\mathbb{C}$. Furthermore, $f_j^O \approx 0$ for $j \in \mathbb{G}$, since GM is surrounded by WM or CSF. Then, we compute the MAP estimator of

$$\Lambda^* = \{\lambda_j^* \,|\, j \in \mathbb{J}\} = \{\lambda_j^G \,|\, j \in \mathbb{G}\} \cup \{\lambda_j \,|\, j \in \mathbb{J} \setminus \mathbb{G}\} \quad (7)$$

such that $E(y_i) = \sum_i c_{ij}^*\lambda_j^*$ with system matrix c_{ij}^* [1]. Propagation of noise in $\mathbb{W}$ and $\mathbb{C}$ is controlled using a Gaussian prior. In $\mathbb{G}$ we use a Gibbs smoothing prior.

III. Experiments

A three-dimensional (3D) realistic software phantom, based on the *BrainWeb* database [2], was constructed. Dimensions are 218×218×30 voxels with an isotropic voxel size of 1 mm. GM, WM and CSF tissues were identified in the "discrete"

Work supported by K.U.Leuven grants IDO-99/005, OT-00/32 and F.W.O. grant G.0174.03.

K. Baete, J. Nuyts and P. Dupont are with Nuclear Medicine, W. Van Paesschen is with Neurology, and P. Suetens is with Medical Image Computing, Radiology-ESAT/PSI, Katholieke Universiteit Leuven, B-3000 Leuven, Belgium. (e-mail: kristof.baete@uz.kuleuven.ac.be)

TABLE I

SIZE AND LOCATION OF THE HYPO-METABOLIC REGIONS AND SNR IN ROI AROUND THE FOUR HYPO-METABOLIC REGIONS. ML-X MEANS POST-SMOOTHED ML USING A 3D GAUSSIAN WITH X MM FWHM.

Hypo-metabolic region	1	2	3	4
Size (cm^3)	1.5	1.2	0.8	1.7
Location	frontal	parietal	temporal	occipital
SNR				
Reconstruction algorithm	ROI 1	ROI 2	ROI 3	ROI 4
ML-4	38.0	31.5	21.1	39.5
ML-5	41.6	33.4	23.0	42.6
ML-6	45.5	35.4	25.2	45.3
ML-7	47.7	36.6	26.6	46.6
ML-8	48.9	37.5	27.4	47.2
A-MAP-1	42.3	37.6	23.9	40.8
A-MAP-2	44.9	37.8	23.5	41.0
A-MAP-3	45.4	36.9	23.2	41.2
A-MAP-2 (1 mm shift)	45.9	38.9	23.3	41.7
A-MAP-2 (1 deg rotation)	45.7	38.2	23.8	42.3

anatomical model [3]. For the baseline phantom, activity was 12.5 counts per voxel (cpv) in GM, 3.125 cpv in WM and 0 cpv in CSF, which corresponds to a realistic count rate. In a duplicate, called the hypo-metabolic phantom, activity in four 3D regions of GM was decreased by 25 % (see Table I).

PET acquisition was simulated by projecting both phantoms over 144 angles using uniform attenuation. Projections were smoothed using a 2D Gaussian with 5 mm full-width at half-maximum (FWHM) to account for the detector resolution and rebinned to 2×2 mm^2 detectors. Of each sinogram 100 Poisson noise realizations were computed and reconstructed using the maximum-likelihood (ML) algorithm. Each reconstruction was post-smoothed using a 3D Gaussian with FWHM varying from 4 to 8 mm. Post-smoothed ML with 4 mm FWHM were used as the initial image for A-MAP. We used attenuation correction and resolution recovery.

Firstly, A-MAP reconstructions were performed using the GM, WM and CSF "fuzzy" tissue classifications provided by the *BrainWeb* database [3] that were rebinned to the PET grid. Dimensions are $109\times109\times15$ voxels with an isotropic voxel size of 2 mm. Emission data and anatomical information are by these means perfectly co-registered. Three different weights of the Gibbs smoothing prior in $\mathbb{G}$ (A-MAP-1, 2, and 3) were used. Secondly, A-MAP-2 reconstructions were performed using mis-registered anatomical information: tissue classification was (a) trans-axially shifted over 1 mm, and (b) rotated over 1 degree, then rebinned to the PET grid. We measured signal-to-noise ratio (SNR) in regions-of-interest (ROI) around the four hypo-metabolic regions [4] and the overall root mean squared (rms) bias and rms standard deviation for the reconstructions based on the baseline phantom. As an example, clinical PET data of an epilepsy patient were reconstructed using A-MAP and post-smoothed ML (4 mm FWHM). Data were pre-corrected for scatter. The anatomy was based on a T1-weighted MR scan of the patient.

IV. RESULTS

Fig. 1 shows rms bias and rms standard deviation results. A-MAP shows a reduction of bias compared to post-smoothed ML. Variation of the prior weight in $\mathbb{G}$ has more effect on standard deviation than on bias. Small mis-registrations have more effect on bias than on standard deviation. SNR results are shown in Table I. A-MAP shows slight improved SNR results, compared to moderate post-smoothed ML. A-MAP shows some robustness for small mis-registrations and for the prior weight in $\mathbb{G}$. Fig. 2 shows promising results of A-MAP compared to post-smoothed ML using clinical PET data.

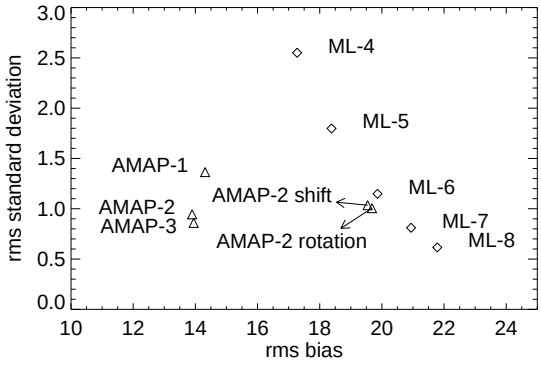

Fig. 1. Root mean squared (rms) bias and rms standard deviation results of the baseline phantom simulations. ML-X means post-smoothed ML using a 3D Gaussian with X mm FWHM.

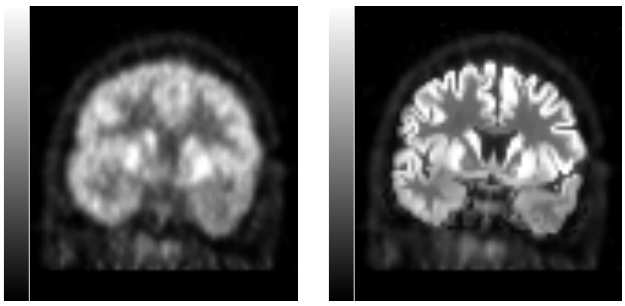

(a) (b)

Fig. 2. Coronal view of clinical PET data of an epilepsy patient reconstructed using (a) post-smoothed ML using a 3D Gaussian with 4 mm FWHM, and (b) A-MAP using anatomical data derived from a T1-weighted MR.

V. CONCLUSION

Anatomical based MAP reconstruction of FDG-PET data shows to be promising for the detection of subtle hypo-metabolic regions in the brain of patients with refractory partial epilepsy.

REFERENCES

[1] K. Baete, J. Nuyts, W. Van Paesschen, P. Suetens, and P. Dupont, "Detection of epileptogenic regions in FDG-PET using anatomical information," *Proc. IEEE Nuc. Sci. Symp. and Med. Imag. Conf.*, M10-94, Norfolk, VA, USA, Nov. 2002.

[2] (2002) BrainWeb. [Online]. Available: www.bic.mni.mcgill.ca/brainweb/

[3] D.L. Collins, A.P. Zijdenbos, V. Kollokian, J.G. Sled, N.J. Kabani, C.J. Holmes, and A.C. Evans, "Design and construction of a realistic digital brain phantom," *IEEE Trans. Med. Imag.*, vol. 17, no. 3, pp. 463–468, Jun. 1998.

[4] H.H. Barrett, J. Yao, J.P. Rolland, and K.J. Myers, "Model observers for assessment of image quality," *Proc. Natl. Acad. Sci. USA*, vol. 90, no. 21, pp. 9758–9765, Nov. 1993.